Figures and figure supplements

Loss of FLCN-FNIP1/2 induces a non-canonical interferon response in human renal tubular epithelial cells

Iris E Glykofridis *et al*

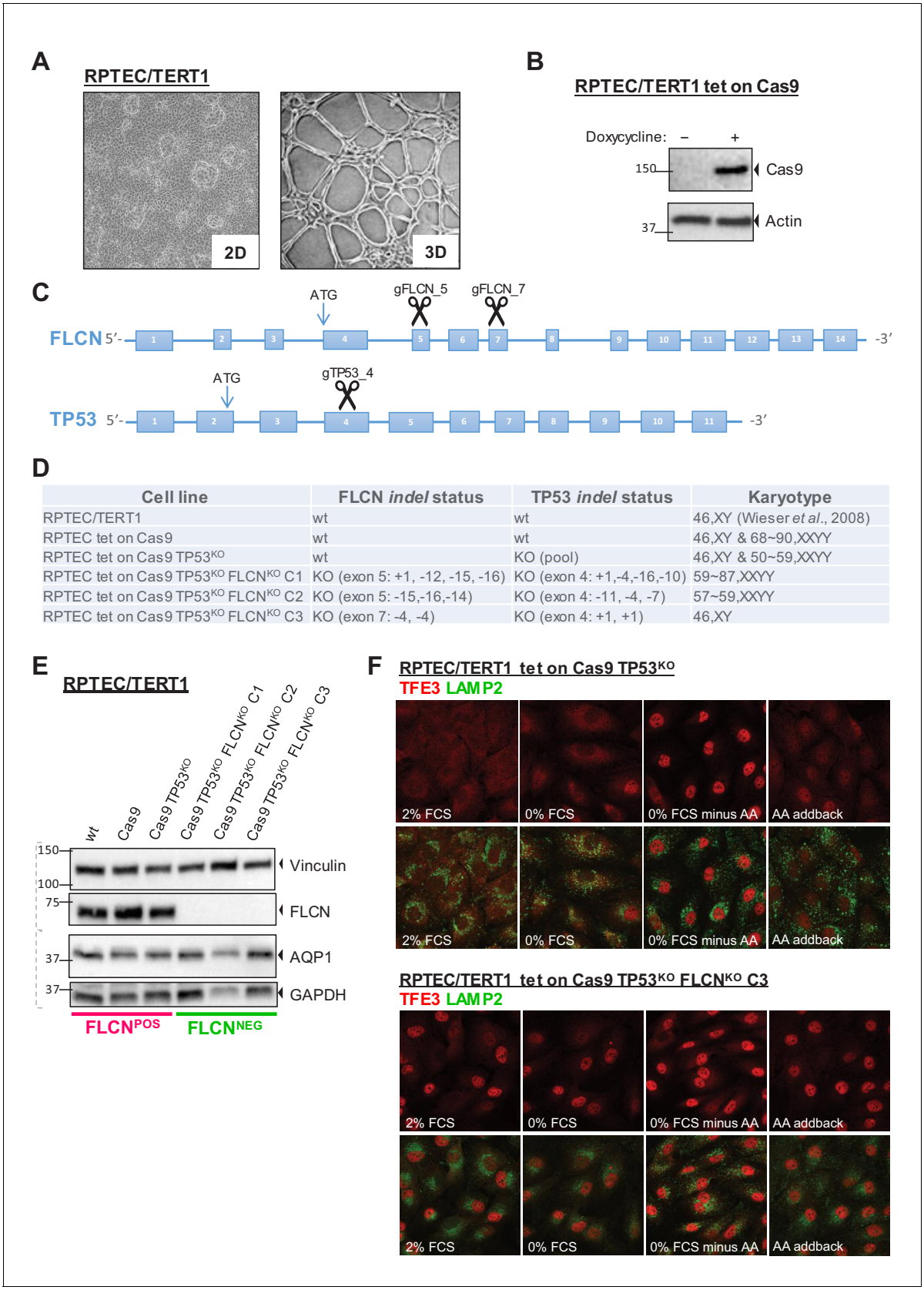

Cell line	FLCN *indel* status	TP53 *indel* status	Karyotype
RPTEC/TERT1	wt	wt	46,XY (Wieser *et al*., 2008)
RPTEC tet on Cas9	wt	wt	46,XY & 68~90,XXYY
RPTEC tet on Cas9 TP53^{KO}	wt	KO (pool)	46,XY & 50~59,XXYY
RPTEC tet on Cas9 TP53^{KO} FLCN^{KO} C1	KO (exon 5: +1, -12, -15, -16)	KO (exon 4: +1,-4,-16,-10)	59~87,XXYY
RPTEC tet on Cas9 TP53^{KO} FLCN^{KO} C2	KO (exon 5: -15,-16,-14)	KO (exon 4: -11, -4, -7)	57~59,XXYY
RPTEC tet on Cas9 TP53^{KO} FLCN^{KO} C3	KO (exon 7: -4, -4)	KO (exon 4: +1, +1)	46,XY

Figure 1. Renal proximal tubular epithelial cells as a model for FLCN loss. (**A**) Brightfield images (×50 magnification) of a human renal proximal tubular epithelial cell model (RPTEC/TERT1). Left image shows 2D culture of cells with typical dome formation. Right image shows 3D tubular structures that

Figure 1 continued on next page

Figure 1 continued

form when RPTECs are cultured according to ***Secker, 2018***. (**B**) Doxycycline-inducible Cas9 expression of RPTEC tet-on Cas9 cell line. Cas9 protein expression after 24 hr treatment with 10 ng/ml doxycycline was assessed by immunoblotting. Experiment was performed twice. (**C**) CRISPR/Cas9-mediated knockout strategy of FLCN and TP53 in RPTEC/TERT1 cells; gRNAs were designed to target early exons of FLCN and TP53 coding regions. (**D**) Overview of *FLCN* and *TP53 indel* status and karyotype per selected cell line clone. Cell-line-specific Sanger sequence chromatograms are shown in ***Figure 1—figure supplement 1A***. (**E**) Western blot of FLCN protein levels of indicated cell line clones. Expression of renal proximal tubular-specific marker AQP1 is shown as a control. Dotted lines indicate separate blots. Western blot of TP53 protein levels is shown in ***Figure 1—figure supplement 1B***. (**F**) Immunofluorescence staining of TFE3 and lysosomal marker LAMP2 show enhanced nuclear TFE3 upon FLCN loss independent of nutrient availability. FCS = fetal calf serum, AA = amino acids. Staining of $FLCN^{KO}$ RPTEC C1 and C2 are shown in ***Figure 1—figure supplement 1C***.

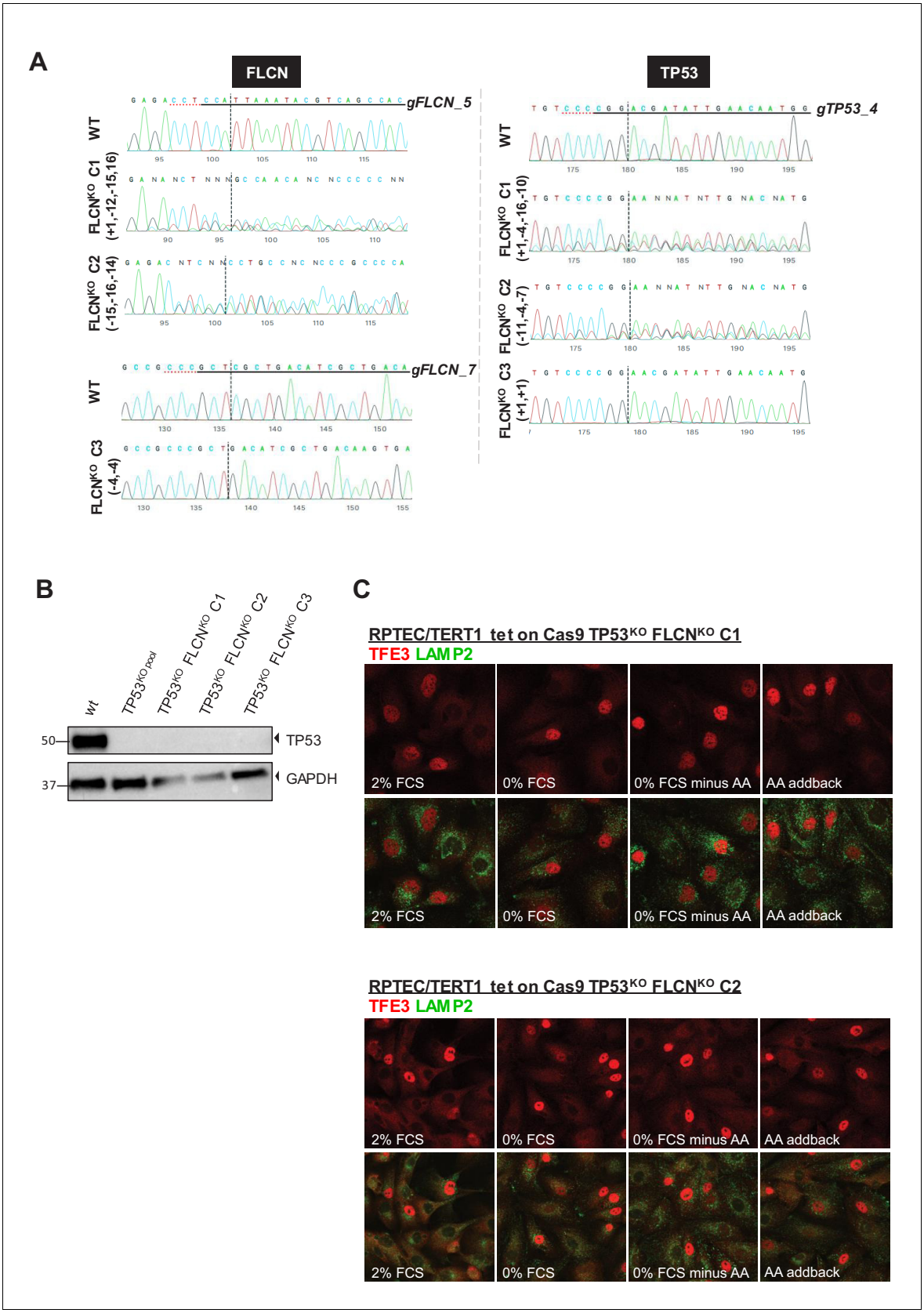

Figure 1—figure supplement 1. Characterization of TP53^{KO} and FLCN^{KO} cell lines. (**A**) Sanger sequence chromatograms of genomic DNA isolated from each modified RPTEC cell line. *Indel* analysis was performed with the on-line Inference of CRISPR Editing (ICE) tool of Synthego. Left column

Figure 1—figure supplement 1 continued on next page

Figure 1—figure supplement 1 continued

shows FLCN sequences, right column shows TP53 sequences. (**B**) Western blot of TP53 protein levels of selected cell line clones upon activation of p53 pathway by Nutlin-3 treatment. Western blot was performed twice. (**C**) Immunofluorescence staining of TFE3 and lysosomal marker LAMP2 show enhanced nuclear TFE3 independent of nutrient availability in $FLCN^{KO}$ clones C1 and C2. FCS = fetal calf serum, AA = amino acids.

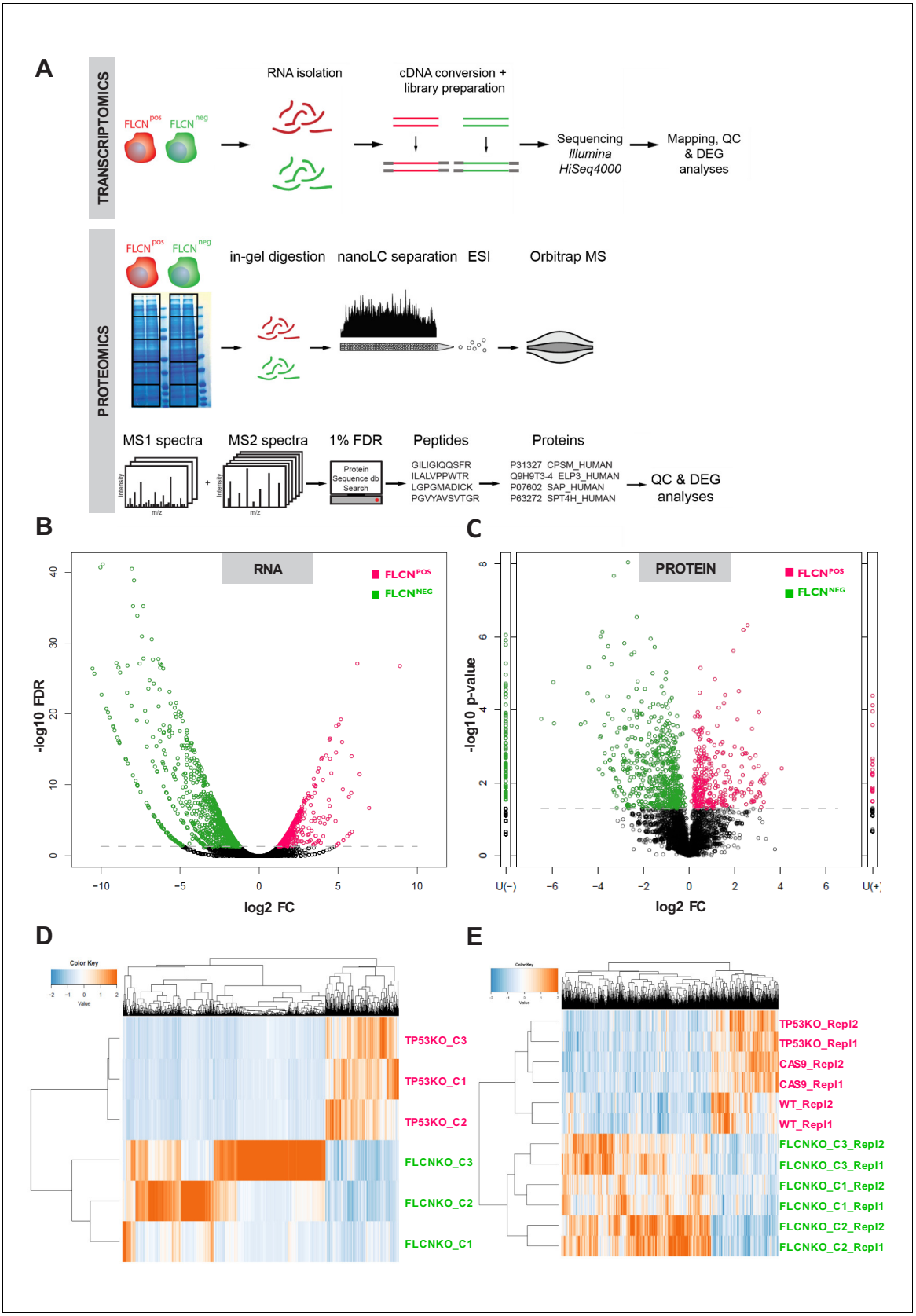

Figure 2. Integrated transcriptomic and proteomic analyses of renal tubular FLCN loss. (**A**) Schematic overview of transcriptomic and proteomic workflows. (**B**) Volcano plot showing significantly increased or decreased expression of genes in $FLCN^{POS}$ vs. $FLCN^{NEG}$ comparison derived from

Figure 2 continued on next page

Figure 2 continued

transcriptomic analysis. Colored circles above threshold line are FDR < 0.05; statistical details can be found in Materials and methods section. (**C**) Volcano plot showing (significantly) increased or decreased expression of proteins in $FLCN^{POS}$ vs. $FLCN^{NEG}$ comparison derived from proteomic analysis. Colored circles above threshold line are $p<0.05$. U(-) column shows proteins uniquely detected in $FLCN^{NEG}$, U(+) column shows proteins uniquely detected in $FLCN^{POS}$. Statistical details can be found in the Materials and methods section. (**D**) Hierarchical clustering based on FLCN-dependent differential mRNA expression. (**E**) Hierarchical clustering based on FLCN-dependent differential protein expression.

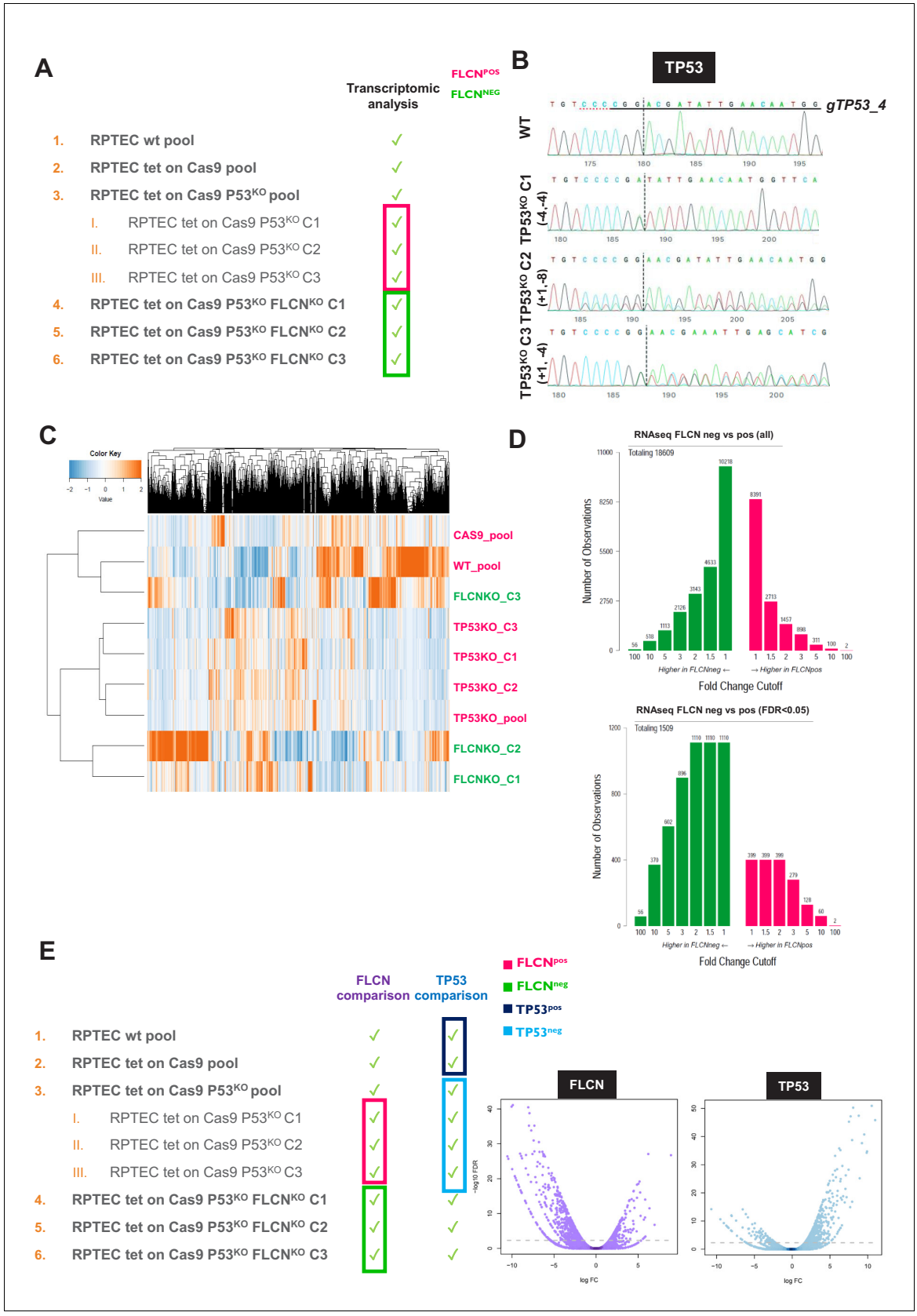

Figure 2—figure supplement 1. Comparative analyses of RPTEC FLCN^{POS} vs. FLCN^{NEG} cell line pairs. (**A**) FLCN^{POS} and FLCN^{NEG} RPTEC cell lines used for RNAseq. To correct for possible clonal effects on global transcription levels, three single-cell clones (C1, C2, and C3 respectively, derived from

Figure 2—figure supplement 1 continued on next page

Figure 2—figure supplement 1 continued

$TP53^{KO}$ pool) were added to the comparison. (**B**) Sanger sequence chromatogram of genomic DNA isolated from $TP53^{KO}$ single cell line clones C1, C2, and C3. *Indel* analysis was performed with the Synthego CRISPR Editing (ICE) tool. (**C**) Unsupervised hierarchical clustering of all genes identified in RNAseq experiment of $FLCN^{POS}$ vs. $FLCN^{NEG}$ RPTEC cell lines (TMM-normalized values). (**D**) Numbers of (significant, FDR < 0.05) differential genes observed in $FLCN^{NEG}$ and $FLCN^{POS}$ RPTECs, ranked by fold change. (**E**) Overview of comparisons made for differential expression analyses. The purple volcano plot represents the $FLCN^{POS}$ vs. $FLCN^{NEG}$ comparison and shows that most significant differentially expressed mRNAs are upregulated in $FLCN^{NEG}$ cells, identifying FLCN as a transcriptional suppressor. The blue volcano represents the $TP53^{POS}$ vs. $TP53^{NEG}$ analysis and shows, for comparison, that loss of the transcriptional activator TP53 reduces expression of the most significant differentially expressed mRNAs. Statistical details can be found in the Materials and methods section.

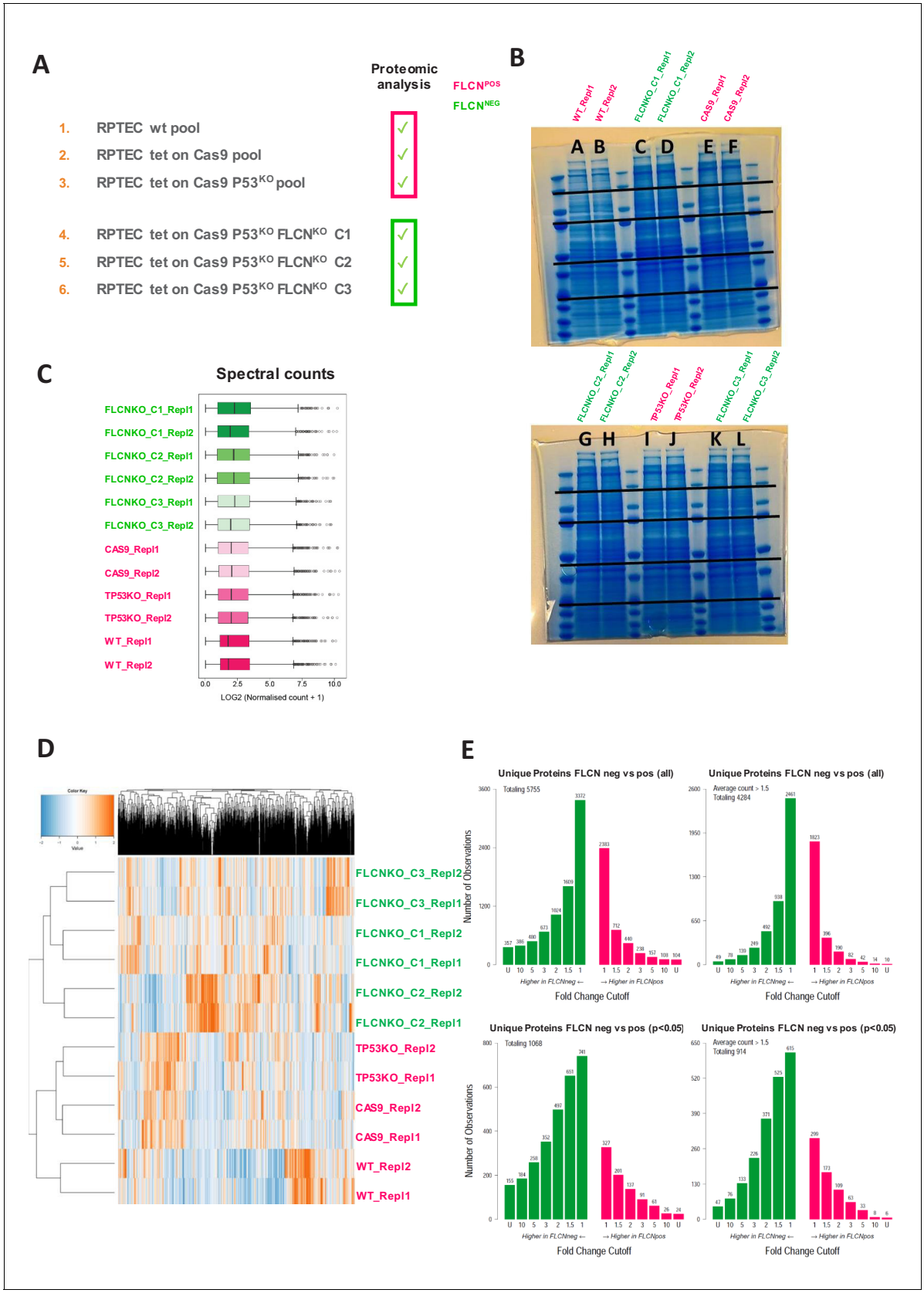

Figure 2—figure supplement 2. GeLC-MS/MS-based proteomics of RPTEC FLCN^{POS} vs. FLCN^{NEG} cell line pairs. (**A**) Cell lines used as input lysates for proteomic analyses FLCN^{POS} vs. FLCN^{NEG} RPTECs. (**B**) Coomassie staining of gel containing samples for proteomic analyses, 5-band fractionation, two

Figure 2—figure supplement 2 continued on next page

Figure 2—figure supplement 2 continued

technical replicates per cell line were measured. (**C**) Overview of the normalized spectral counts per cell line. (**D**) Unsupervised hierarchical clustering of all proteins identified in MS experiment (normalized counts). (**E**) Numbers of all (top plots) or $p<0.05$ (lower plots) differential proteins observed in $FLCN^{NEG}$ or $FLCN^{POS}$ RPTECs, ranked by fold change. Left: no threshold counts; right: average count >1,5. The data show upregulated protein expression by FLCN loss. Statistical details can be found in Materials and methods section.

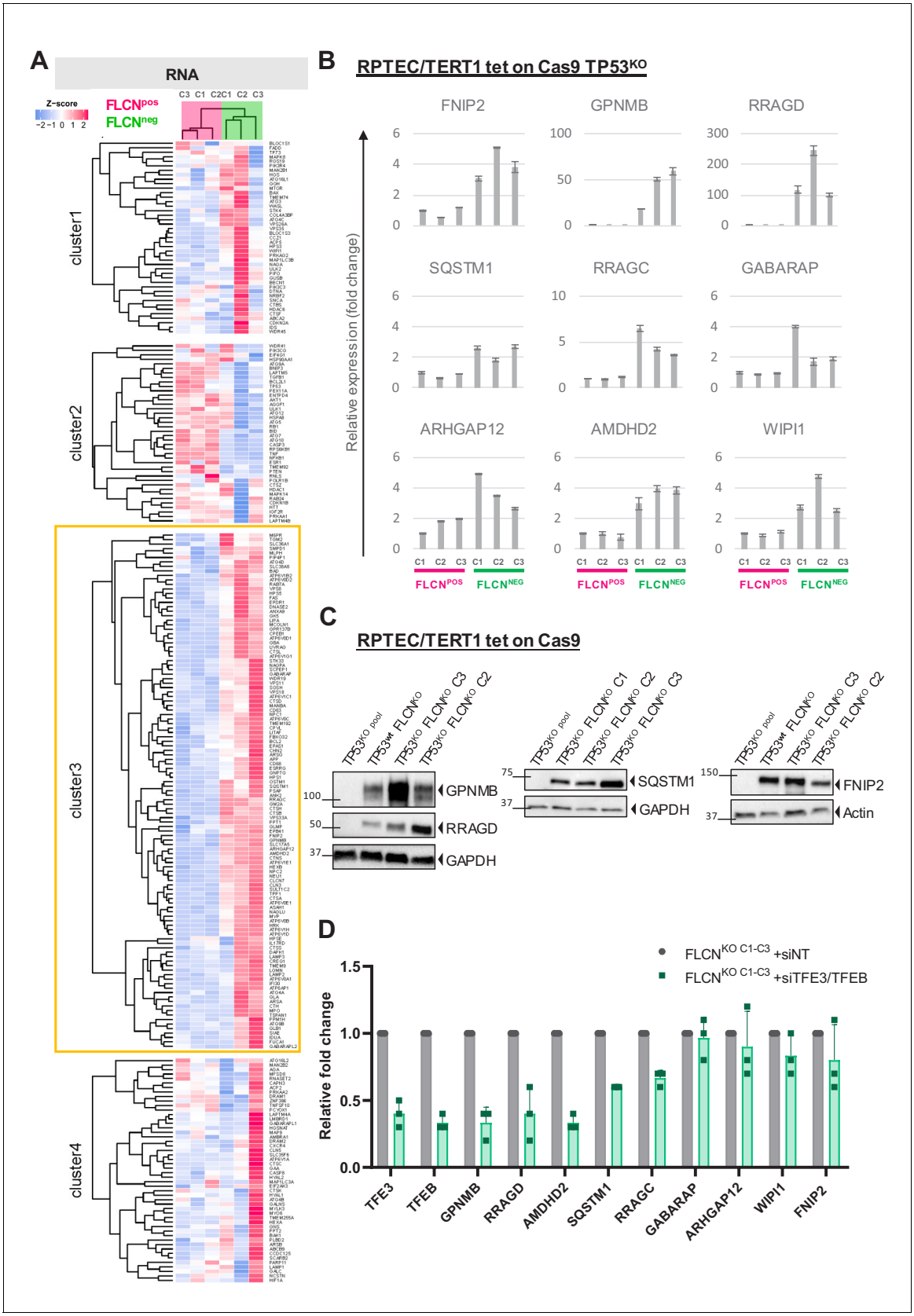

Figure 3. FLCN loss results in upregulation of subset of TFE target genes. (**A**) Heat map showing k-means Pearson correlation clustering of TMM-normalized RNAseq data of FLCN^{pos} versus FLCN^{neg} RPTECs. We analyzed published TFEB/TFE3 target genes. Yellow boxed cluster three shows the

Figure 3 continued on next page

Figure 3 continued

subset (n = 115) of TFEB/TFE3 targets upregulated in all three $FLCN^{NEG}$ clones. (**B**) Upregulation of TFE target genes FNIP2, GPNMB, RRAGD, SQSTM1, RRAGC, GABARAP, ARHGAP12, AMDHD2, and WIPI1 in $FLCN^{NEG}$ RPTECs. Results of three independent experiments with three technical replicates. To determine quantitative gene expression levels, data were normalized to the geometric mean of two housekeeping genes. See ***Figure 3—source data 1*** for raw qRT-PCR values and fold change calculations. (**C**) Western blots of RPTEC/TERT1 tet-on Cas9 cell lines. All $FLCN^{NEG}$ clones show strong induction of protein expression of TFE targets GPNMB, RRAGD, SQSTM1, and FNIP2. GAPDH and Actin were used as loading controls. Western blots were performed three times. (**D**) Knock down of TFE3/TFEB (10 nM siRNA, 72 hr) ameliorates the TFE expression gene signature induced by FLCN loss in three $FLCN^{NEG}$ clones. Expression levels were determined by qRT-PCR, normalized to siNT-treated clones and are representative of three independent experiments. To determine quantitative gene expression data levels were normalized to the geometric mean of two housekeeping genes. Also see ***Figure 8—figure supplement 1C***. Effects of siTFE3 alone are shown in ***Figure 3—figure supplement 1C***. See ***Figure 3—source data 1*** for raw qRT-PCR values and fold change calculations.

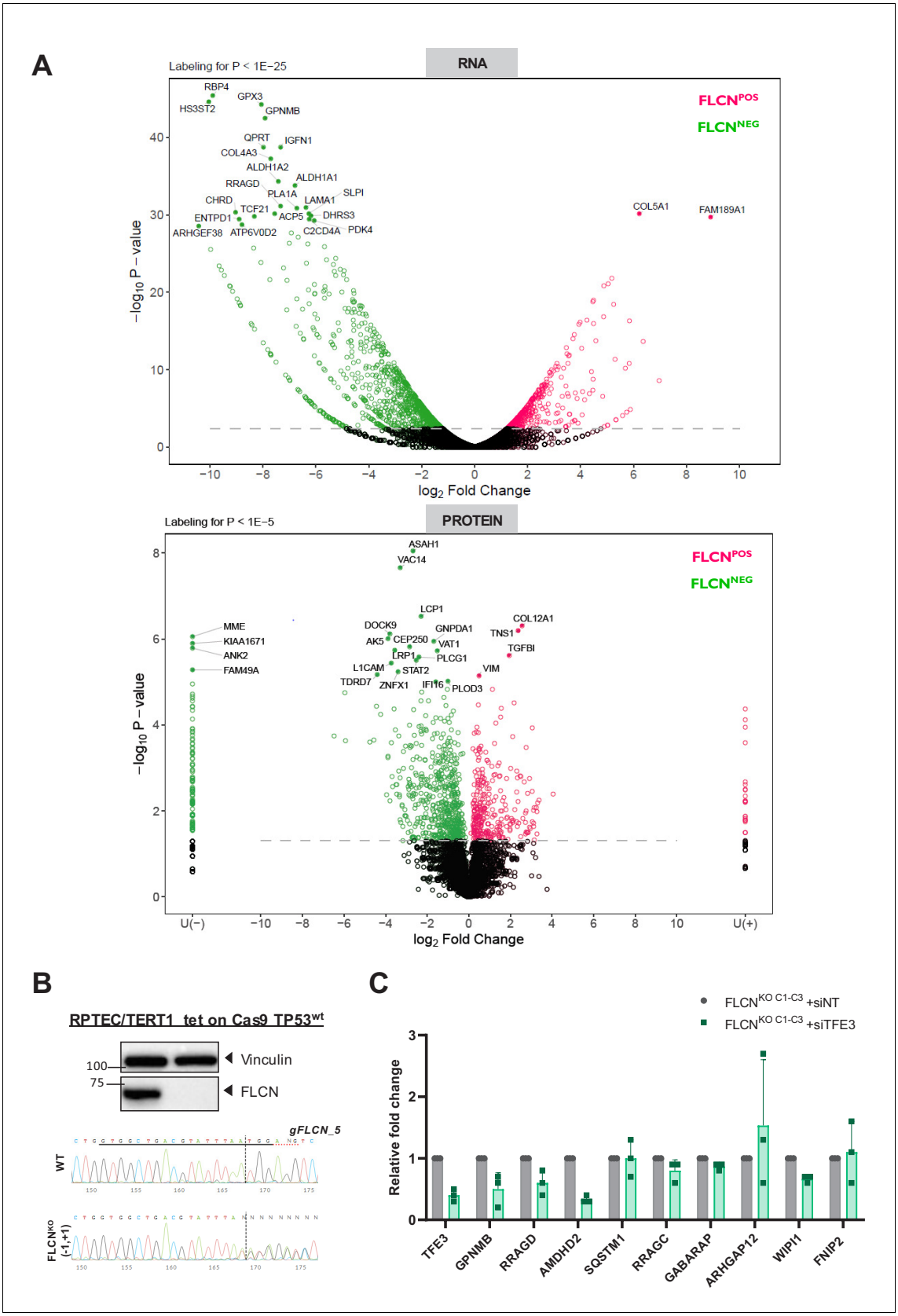

Figure 3—figure supplement 1. Comparative analyses of RPTEC FLCN^{POS} vs. FLCN^{NEG} cell line pairs and validations of TP53^{WT} FLCN^{KO} RPTEC cell line. (**A**) Similar volcano plots are shown as described in ***Figure 2B and C***, while here the most significant genes for RNA (p-value<1 ~ E-25) and protein

Figure 3—figure supplement 1 continued on next page

Figure 3—figure supplement 1 continued

(p-value<1E-5) are annotated. Statistical details can be found in the materials and methods section. (**B**) Western blot and Sanger sequence chromatogram confirm FLCN knockout in RPTEC tet on Cas9 $TP53^{WT}$ cell line. Vinculin was used as a loading control and western blot was performed three times. (**C**) Knock down of TFE3 (siRNA, 10 nM, 72 hr) in three $FLCN^{NEG}$ clones. Expression levels were determined by qRT-PCR, normalized to siNT-treated clones and are representative of three independent experiments. To determine quantitative gene expression data levels were normalized to the geometric mean of two housekeeping genes. See ***Figure 3—source data 1*** for raw qRT-PCR values and fold change calculations.

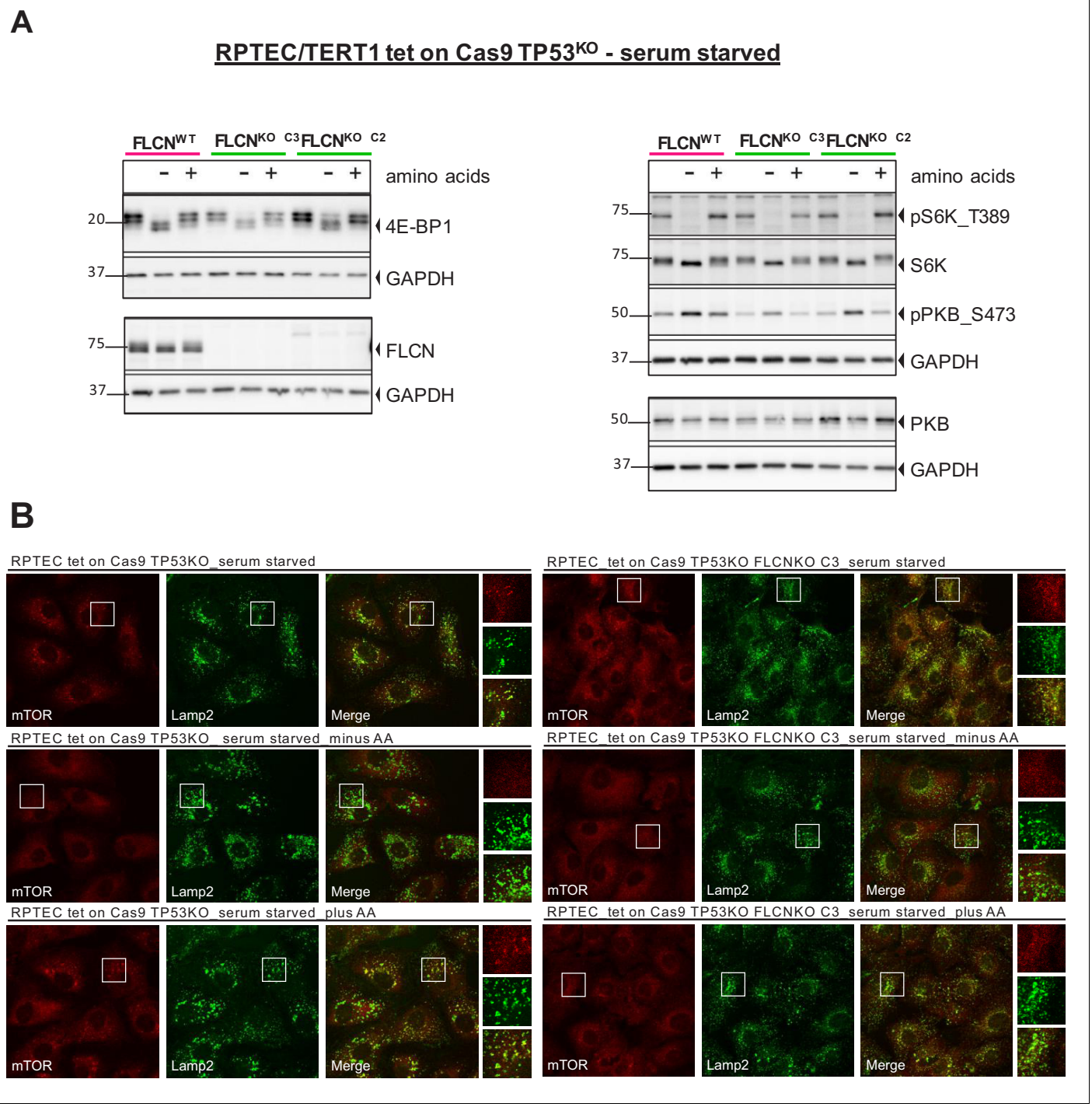

Figure 4. mTOR localization and signaling in response to starvation does not change upon FLCN loss in RPTEC. (**A**) To detect changes in canonical mTOR signaling, phosphorylation levels of S6 kinase (S6K_T389) and AKT/PKB (PKB_S473) and total protein levels of S6K, AKT/PKB, 4E-BP1 were assessed by western blot. Serum starved FLCN^{POS} and FLCN^{NEG} RPTEC cell lines with and without additional amino acids (AA) depletion were analyzed three times. (**B**) Immunofluorescence staining of mTOR and lysosomal marker LAMP2 show no FLCN dependent difference of mTOR localization in response to starvation. FCS = fetal calf serum, AA = amino acids. Staining of FLCN^{NEG} RPTEC C3 is representative for three independent FLCN^{NEG} clones.

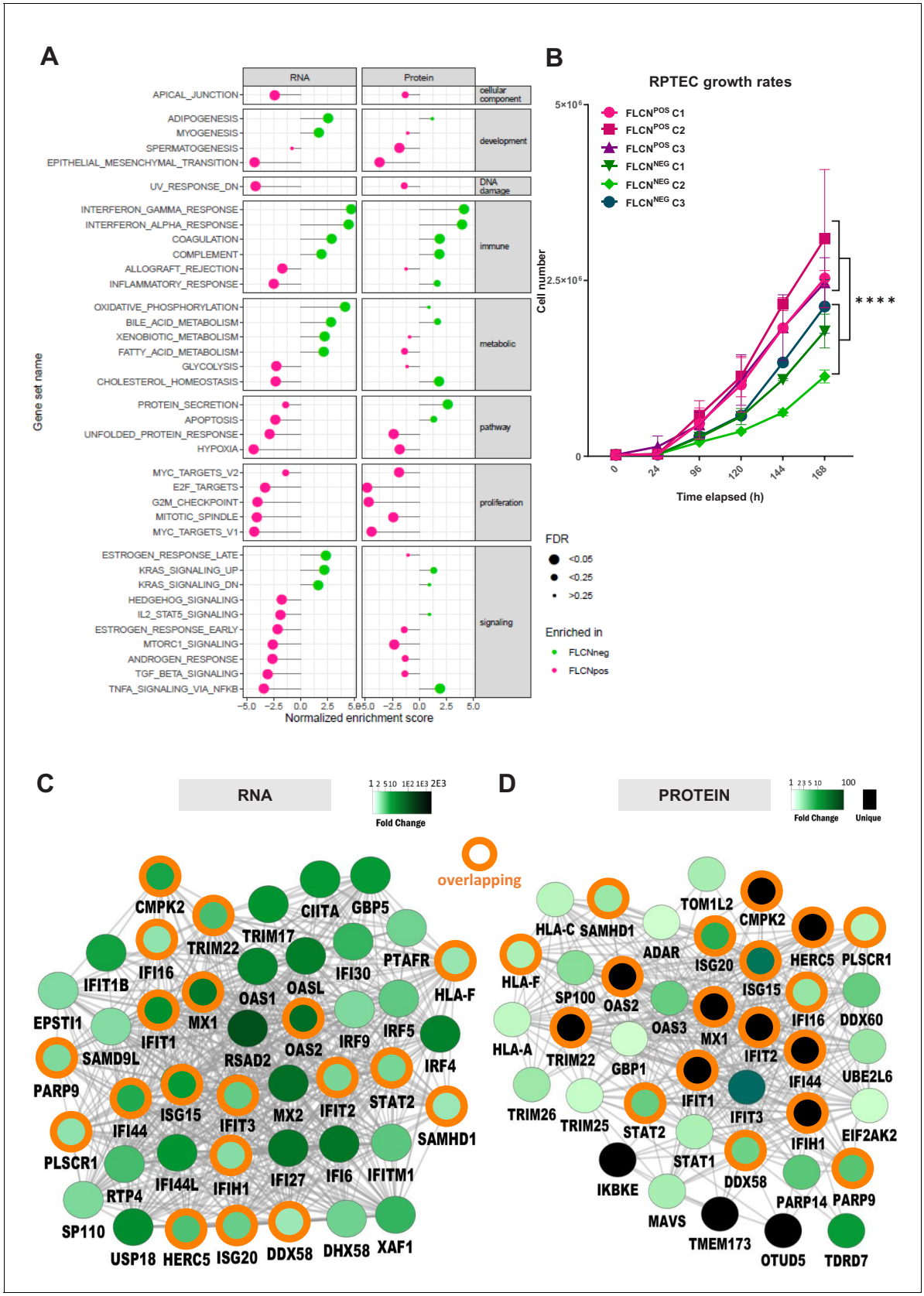

Figure 5. Gene set enrichment analysis reveals FLCN-dependent biological processes. (**A**) For Gene Set Enrichment Analysis (GSEA) genes or proteins were ranked based on p-values, with genes/proteins that are expressed significantly higher in FLCN^{NEG} RPTECs shown on top of the list (hallmark gene

Figure 5 continued on next page

Figure 5 continued

sets, classic ES). Enriched hallmark gene sets are ranked by normalized enrichment score (NES). Gene sets enriched in $FLCN^{NEG}$ are shown in green and gene sets enriched in $FLCN^{POS}$ in pink. The size of the dot reflects the significance of the enrichment (FDR=false discovery rate). Only biological processes that were significant in either RNA and/or protein data are depicted in this Figure. An extended version with all identified gene sets is shown in ***Figure 6—figure supplement 1A***. (**B**) $FLCN^{NEG}$ RPTECs grow significantly slower (p=8.31E-11) when compared to $FLCN^{POS}$ RPTEC. Cell lines were seeded in equal densities and total cell number was counted for 7 consecutive days. Results shown are representative for two independent experiments. (**C**) Gene Ontology (biological processes, BinGO) analysis of mRNAs higher expressed in $FLCN^{NEG}$ RPTECs reveals highly overlapping (orange circles) clusters of immune- and interferon-response-related genes between both data sets. Shade of green nodes represents fold change. (**D**) Gene Ontology (biological processes, BinGO) analysis of proteins higher expressed in $FLCN^{NEG}$ RPTECs reveals highly overlapping (orange circles) clusters of immune and interferon response related genes between both data sets. Shades of green nodes represent different levels of fold change. Black nodes indicate uniquely detected proteins in $FLCN^{NEG}$ RPTEC.

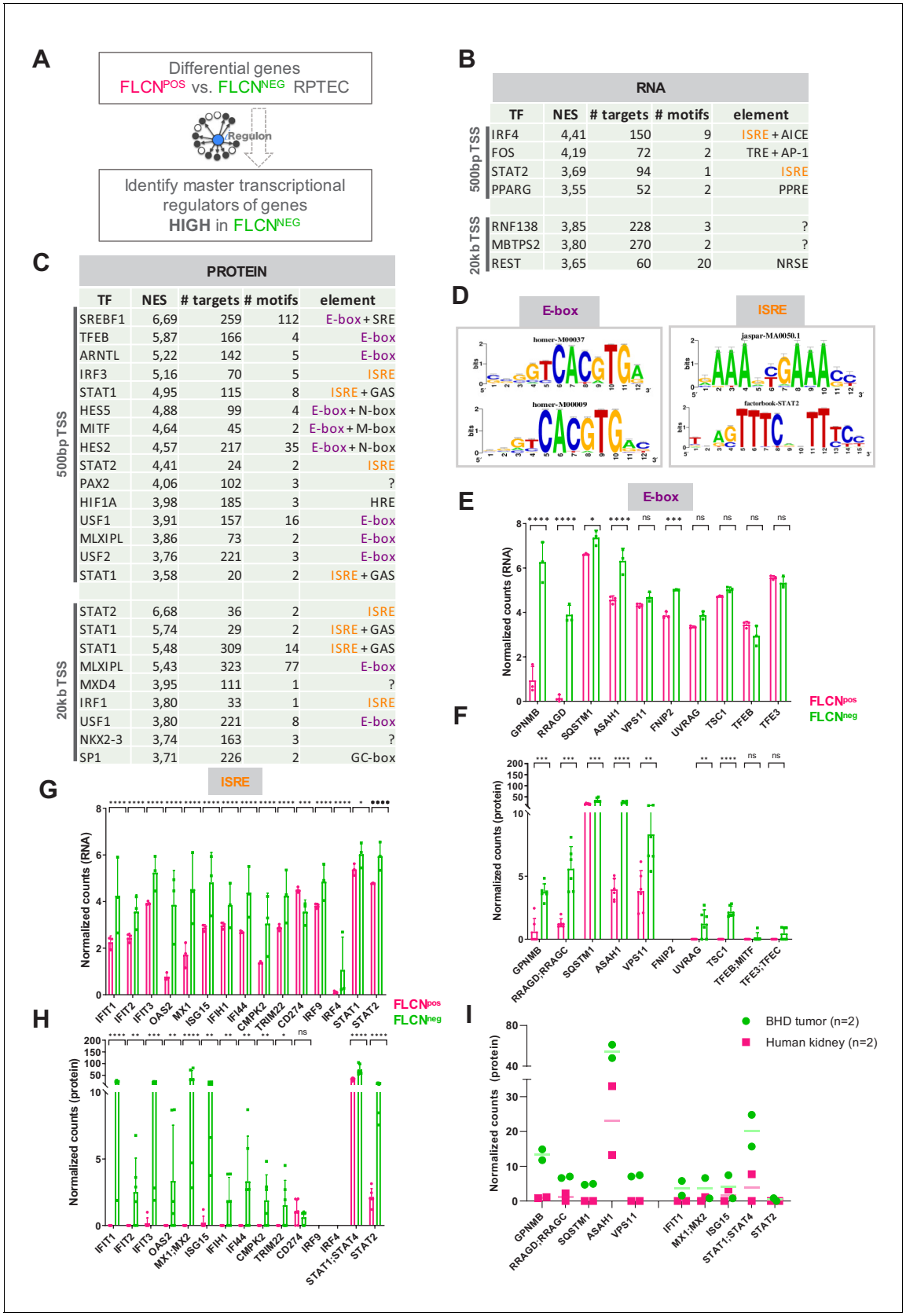

Figure 6. Identification of regulatory elements activated by FLCN loss in RPTEC and BHD tumors. (**A**) Identification of transcriptional regulatory elements associated with loss of FLCN expression. Regulons were identified by iRegulon (***Janky et al., 2014***), using an input a list of differential

Figure 6 continued on next page

Figure 6 continued

expressed genes (***Figure 3***). (**B**) Upstream regulons enriched in $FLCN^{NEG}$ RPTEC based on significantly upregulated genes derived from our transcriptomic data set (n = 711, FDR < 0.05 and logFC > 2). Transcription factors with normalized enrichment scores (NES) higher than 3.5 are shown, together with detected number of targets, motifs, and elements. ISREs are highlighted in orange. Upper part shows motifs enriched 500 bp upstream from transcription start site (TSS), lower part shows motifs enriched 20 kb around TSS. (**C**) Upstream regulons enriched in $FLCN^{NEG}$ RPTEC based on significantly upregulated proteins derived from our proteomic data set (n = 498, p<0.05 and FC > 2). Transcription factors with normalized enrichment score (NES) higher than 3.5 are shown, together with number of targets, motifs, and elements detected. ISREs are highlighted in orange and E-boxes in purple. STAT1 appears twice due to the fact that iRegulon ranks this transcription factor to be the most likely upstream regulator for two sets of targets genes, containing slightly different ISRE-motifs 20 kb upstream from the TSS. (**D**) Two major enriched motif elements detected in iRegulon analysis of genes upregulated in $FLCN^{NEG}$ RPTEC. Regulons can be assigned to E-box (in purple) or ISRE (in orange) motif group. (**E**) Bar graphs of RNA expression levels of genes associated with an E-box motif, derived from RPTEC transcriptomic data set. $FLCN^{POS}$ values are shown in pink and $FLCN^{NEG}$ values are shown in green. Significant p-values are indicated as *≤0.05, **≤0.01, ***≤0.001, ****≤0.0001. (**F**) Bar graphs of protein expression levels of genes associated with an E-box motif, derived from RPTEC proteomic data set. $FLCN^{POS}$ values are shown in pink and $FLCN^{NEG}$ values are shown in green. FNIP2 peptides were not detected in our proteomic experiment and therefore absent in the bar graph. Significant p-values are indicated as *≤0.05, **≤0.01, ***≤0.001, ****≤0.0001. (**G**) Bar graphs of RNA expression levels of genes associated with an ISRE motif derived from RPTEC transcriptomic data set. $FLCN^{POS}$ values are shown in pink and $FLCN^{NEG}$ values are shown in green. Significant p-values are indicated as *≤0.05, **≤0.01, ***≤0.001, ****≤0.0001. (**H**) Bar graphs of protein expression levels of genes associated with an ISRE motif derived from RPTEC proteomic data set. $FLCN^{POS}$ values are shown in pink and $FLCN^{NEG}$ values are shown in green. IRF9 and IRF4 peptides were not detected in our proteomic experiment and therefore absent in the bar graph. Significant p-values are indicated as *≤0.05, **≤0.01, ***≤0.001, ****≤0.0001. (**I**) Dot plot of protein expression levels of genes associated with an E-box (left) or ISRE motif (right) derived from BHD kidney tumor proteomic data sets (see ***Figure 6—figure supplement 1D and E***), as compared to normal kidney tissue. $FLCN^{POS}$ values are shown in pink and $FLCN^{NEG}$ values are shown in green. STAT2 levels were below detection levels in these protein extracts.

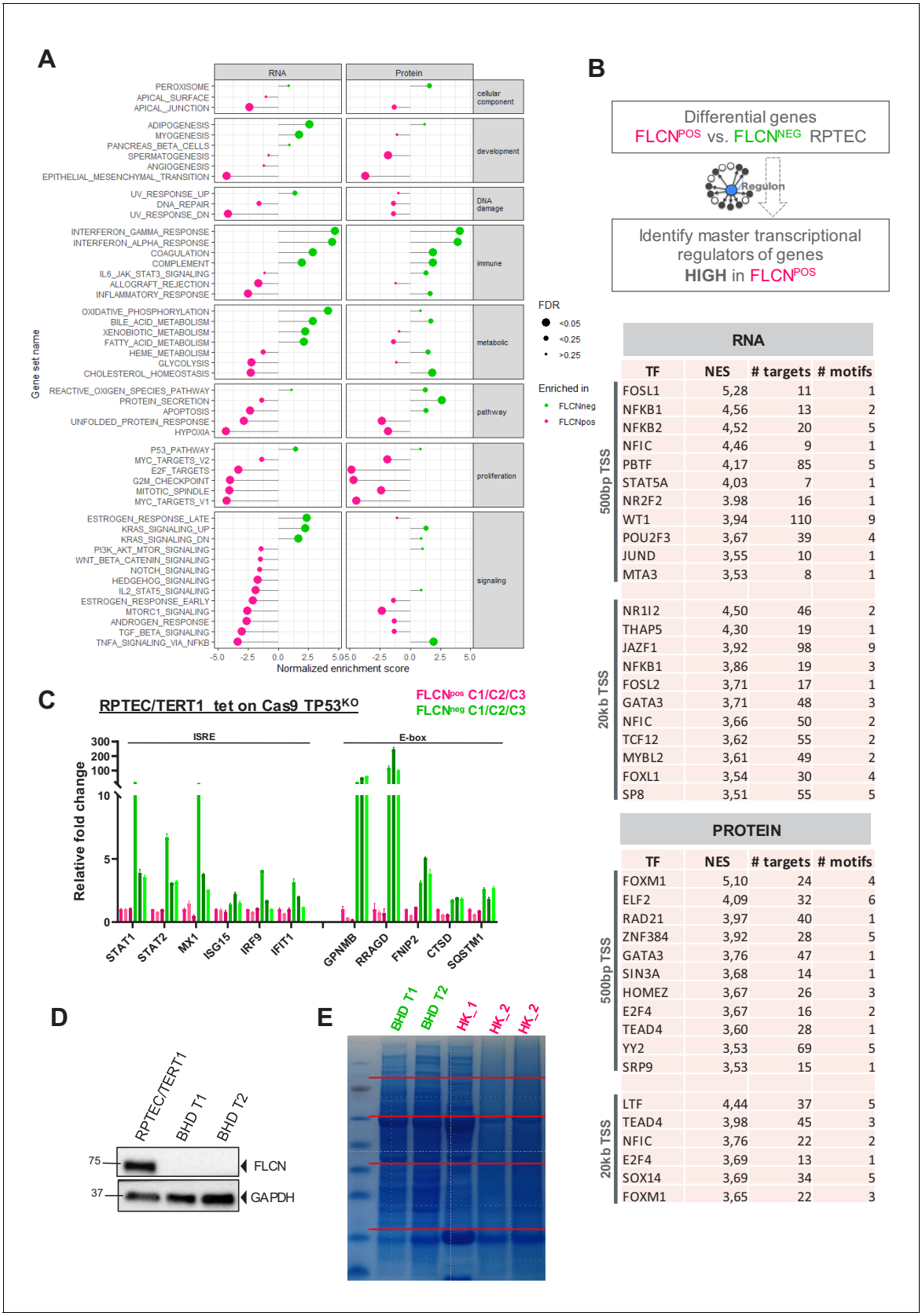

RNA

	TF	NES	# targets	# motifs
500bp TSS	FOSL1	5,28	11	1
	NFKB1	4,56	13	2
	NFKB2	4,52	20	5
	NFIC	4,46	9	1
	PBTF	4,17	85	5
	STAT5A	4,03	7	1
	NR2F2	3.98	16	1
	WT1	3,94	110	9
	POU2F3	3,67	39	4
	JUND	3,55	10	1
	MTA3	3,53	8	1
20kb TSS	NR1I2	4,50	46	2
	THAP5	4,30	19	1
	JAZF1	3,92	98	9
	NFKB1	3,86	19	3
	FOSL2	3,71	17	1
	GATA3	3,71	48	3
	NFIC	3,66	50	2
	TCF12	3,62	55	2
	MYBL2	3,61	49	2
	FOXL1	3,54	30	4
	SP8	3,51	55	5

PROTEIN

	TF	NES	# targets	# motifs
500bp TSS	FOXM1	5,10	24	4
	ELF2	4,09	32	6
	RAD21	3,97	40	1
	ZNF384	3,92	28	5
	GATA3	3,76	47	1
	SIN3A	3,68	14	1
	HOMEZ	3,67	26	3
	E2F4	3,67	16	2
	TEAD4	3,60	28	1
	YY2	3,53	69	5
	SRP9	3,53	15	1
20kb TSS	LTF	4,44	37	5
	TEAD4	3,98	45	3
	NFIC	3,76	22	2
	E2F4	3,69	13	1
	SOX14	3,69	34	5
	FOXM1	3,65	22	3

Figure 6—figure supplement 1. Extended GSEA and iRegulon analysis of FLCN loss in RPTEC and BHD tumors. (**A**) For Gene Set Enrichment Analysis (GSEA) genes or proteins were ranked based on p-values, with genes/proteins significantly higher expressed in FLCN^{NEG} RPTEC on top of the list

Figure 6—figure supplement 1 continued on next page

Figure 6—figure supplement 1 continued

(hallmark gene sets, classic ES). Enriched hallmark gene sets are ranked by normalized enrichment score (NES), with gene sets enriched in $FLCN^{NEG}$ marked in green and gene sets enriched in $FLCN^{POS}$ marked pink. The size of the dot reflects the significance of the enrichment (FDR=false discovery rate). (**B**) Identification of master transcriptional regulators associated with FLCN expression. Regulons were identified with iRegulon tool (***Janky et al., 2014***), using an input a list of FLCN differential expressed genes derived from our transcriptomic and proteomic analyses (***Figures 2*** and ***3***). Tables showing upstream regulons enriched in $FLCN^{POS}$ RPTEC based on significantly upregulated genes (n = 62, FDR < 0.05 and logFC > 2) and proteins (n = 138, p<0.05 and FC > 2). Transcription factors with normalized enrichment score (NES) higher than 3.5 are shown, together with detected number of targets, motifs, and elements. Upper part of table shows motifs enriched 500 bp upstream from transcription start site (TSS), lower part shows motifs enriched 20 kb around TSS. (**C**) Upregulation of target genes with an ISRE or E-box motif in $FLCN^{NEG}$ RPTEC cell lines was validated by qRT-PCR. Results shown are representative for three independent experiments with three technical replicates. To determine quantitative gene expression, data levels were normalized to the geometric mean of two housekeeping genes. See ***Figure 6—figure supplement 1—source data 1*** for raw qRT-PCR values and fold change calculations. (**D**) Absence of FLCN protein expression in two BHD tumors (BHD T1 and BHD T2) was verified by western blotting. GAPDH was used as loading control and western blot was performed three times. (**E**) Coomassie staining of gel containing samples for proteomic analyses of BHD T1, BHD T2 and two normal kidney lysates (HK_1 and HK_2). For measurements, 5-band fractionation was applied to all samples and two lanes of HK_2 were combined.

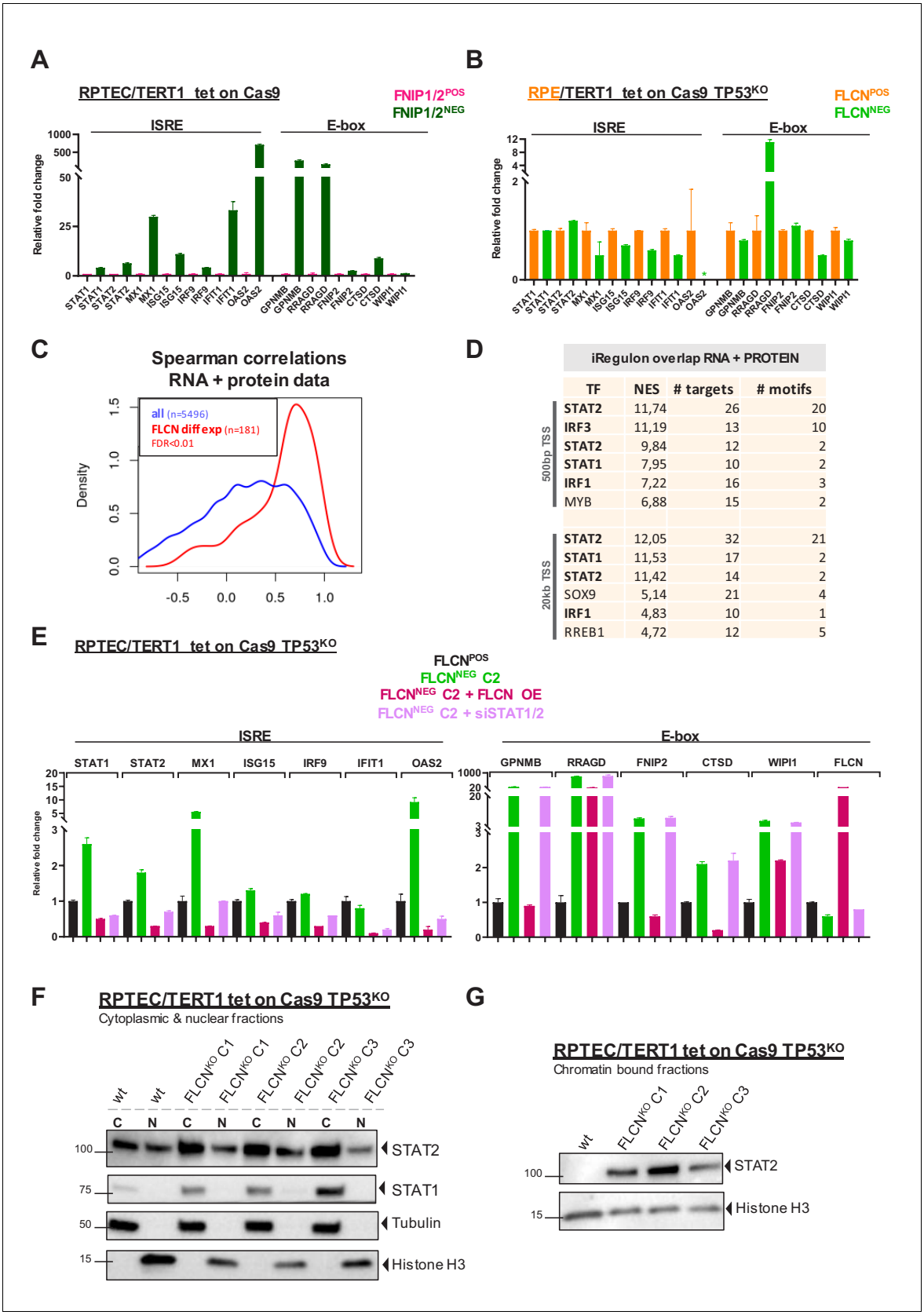

Figure 7. Inactivation of the FLCN-FNIP1/2 axis activates STAT2 in renal cells. (**A**) qRT-PCR levels of genes with ISRE or E-box motif in FNIP1^{POS}/FNIP2^{POS} and FNIP1^{NEG}/FNIP2^{NEG} RPTEC cells reveal that the identified FLCN-dependent gene signature is also induced upon loss of FLCN

Figure 7 continued on next page

Figure 7 continued

interacting proteins FNIP1 and FNIP2. Results shown are representative for two independent experiments with three technical replicates. To determine quantitative gene expression data levels were normalized to the geometric mean of two housekeeping genes. See ***Figure 7—source data 1*** for raw qRT-PCR values and fold change calculations. (**B**) qRT-PCR levels of genes with ISRE or E-box motif in $FLCN^{POS}$ and $FLCN^{NEG}$ retinal pigment epithelial cells (RPE/TERT1 tet on Cas9 $TP53^{KO}$) reveal that the identified FLCN dependent gene signature is absent in an epithelial cell type of another tissue origin. Results shown are representative for two independent experiments. To determine quantitative gene expression data levels were normalized to the geometric mean of two housekeeping genes. *OAS2 level in $FLCN^{NEG}$ RPE was too low to detect using qRT-PCR. See ***Figure 7—source data 1*** for raw qRT-PCR values and fold change calculations. (**C**) Spearman correlation analysis reveals overlapping FLCN-dependent RNA and protein data. FLCN differential mRNAs and proteins (FDR < 0.01, n = 181, red line) showed a higher correlation than the overlap of all identified mRNAs and proteins in our datasets (blue line). Statistical methods are described in Materials and methods section. (**D**) iRegulon analysis of differentially expressed genes (FDR < 0.01) with highest correlation with differentially expressed proteins (r > 0.8, n = 49) reveal STAT1, STAT2, IRF1, and IRF3 as most obvious upstream transcriptional regulators. Only regulons displaying normalized enrichment scores (NES) > 4.5 are shown. STAT2 appears twice due to the fact that iRegulon ranks this transcription factor to be the most likely upstream regulator for two sets of targets genes, containing slightly different ISRE-motifs upstream from the transcription start site (TSS). (**E**) Reintroducing FLCN (overexpression, OE) or siRNA-mediated knock down of STAT1/STAT2 (10 nM, 72 hr) revert the IFN expression gene signature induced by FLCN loss in RPTEC $FLCN^{NEG}$ C2. FLCN OE also lowers the enhanced expression of E-box-associated target genes but knock down of STAT1/2 has no effect on E-box-associated genes. Expression levels were determined by qRT-PCR and are representative of two independent experiments. To determine quantitative gene expression data levels were normalized to the geometric mean of two housekeeping genes. See ***Figure 7—source data 1*** for raw qRT-PCR values and fold change calculations. (**F**) Western blots of subcellular fractionated samples show higher expression of STAT1 and STAT2 in $FLCN^{NEG}$ RPTEC as compared to $FLCN^{POS}$ RPTEC. STAT2 was also detected in both cytoplasmic and nuclear fractions. Tubulin and histone H3 levels were used as loading control and to distinguish each fraction (N=nuclear, C=cytoplasmic). Results shown are representative of two independent fractionations. (**G**) Western blot of subcellular fractionated samples shows enhanced STAT2 DNA binding in $FLCN^{NEG}$ RPTEC. Results shown are representative of three independent fractionations.

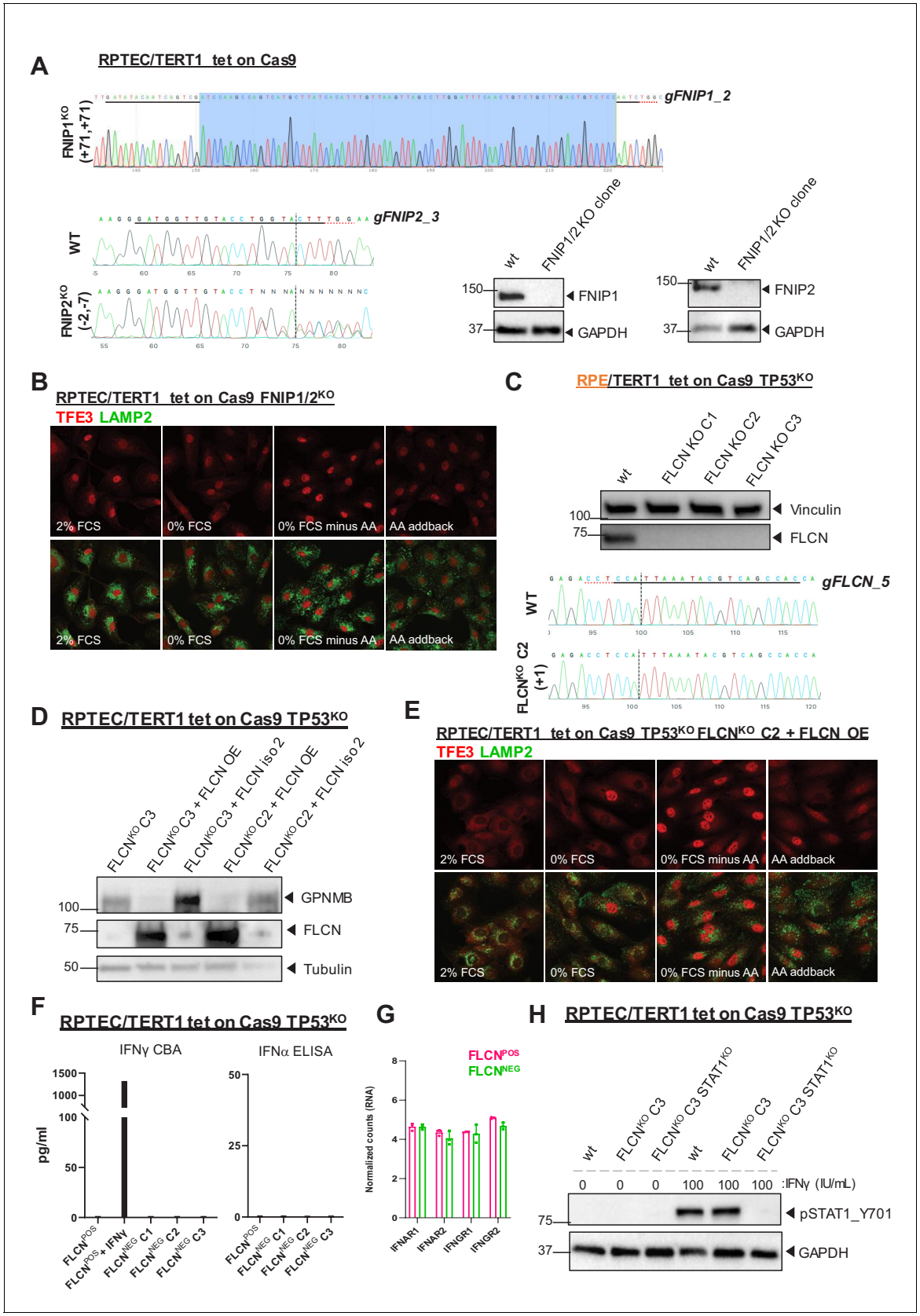

Figure 7—figure supplement 1. Validation of FLCNs role in the IFN response in additional cell models. (**A**) Validation of *FNIP1/FNIP2* knock out in RPTEC/TERT1 tet-on Cas9 TP53^{KO} cells by FNIP1 and FNIP2 sequencing and immunoblotting. Sanger sequence chromatograms of genomic DNA

Figure 7—figure supplement 1 continued on next page

Figure 7—figure supplement 1 continued

isolated from FNIP1^{wt} /FNIP2^{wt} and FNIP1^{KO}/FNIP2^{KO} RPTEC cell lines. *Indel* analysis for *FNIP2* was performed with the on-line ICE tool of Synthego. FNIP1 sequence chromatograms were aligned and revealed a homozygous insertion of 71 nucleotides in FNIP1^{KO}. (**B**) Immunofluorescence staining of TFE3 and lysosomal marker LAMP2 show enhanced nuclear TFE3 upon FNIP1/2 loss independent of nutrient availability. FCS = fetal calf serum, AA = amino acids. (**C**) Validation of FLCN knock out in retinal pigment epithelial cells (RPE/TERT1 tet on Cas TP53^{KO}) by immunoblot and sequencing. Clone two was used for further validations. Sanger sequence chromatograms of genomic DNA isolated from FLCN^{wt} and FLCN^{KO} C2 RPE cell line. *Indel* analysis was performed with the on-line Inference of CRISPR Editing (ICE) tool of Synthego. (**D**) Validation of FLCN isoform one re-expression in RPTEC tet on Cas9 TP53^{KO} FLCN^{KO} C2 and C3 by immunoblot. Higher protein expression of E-box associated target GPNMB was reverted upon restored FLCN expression. Tubulin was used as loading control and western blot was performed twice. Re-expression of FLCN isoform two did not revert the phenotype. (**E**) Immunofluorescence staining of TFE3 and lysosomal marker LAMP2 show rescue of TFE3 nuclear localization and responsiveness on nutrient availability when FLCN expression is restored in FLCN^{NEG} RPTEC C2. FCS = fetal calf serum, AA = amino acids. (**F**) IFNγ Cytometric Bead Array (CBA) or IFNα ELISA detect no FLCN-dependent alterations of both cytokines in supernatant of FLCN^{POS} and FLCN^{NEG} RPTEC cells. Results shown are representative for two independent experiments. (**G**) Bar graphs of RNA expression levels (derived from our transcriptomic data) of IFN receptor genes show no differential expression between FLCN^{POS} versus FLCN^{NEG} RPTEC cell lines. (**H**) Western blot of pSTAT1_Y701 shows no induction of canonical IFN signaling in FLCN^{NEG} RPTEC. As positive control, cell lines were treated with 100IU/ml IFNγ for 1 hr. GAPDH was used as loading control. A STAT1^{KO} RPTEC was taken along as negative control.

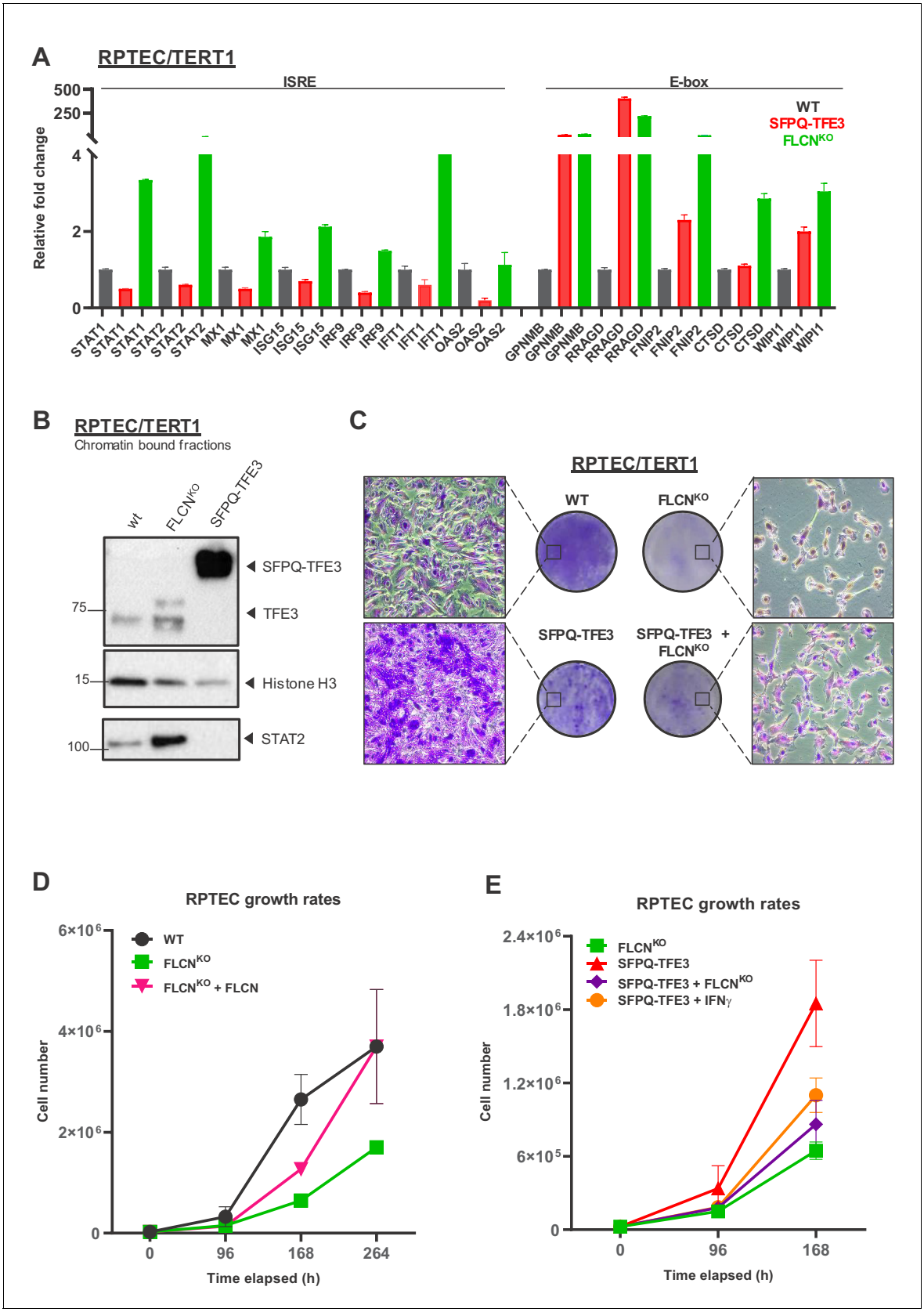

Figure 8. FLCN loss induces an interferon signature which counteracts growth promoting effects of active TFE3 in renal tubular cells. (**A**) Expression of a constitutively active SFPQ-TFE3 fusion protein in RPTEC results in upregulation of E-box-associated targets but does not induce enhanced expression

Figure 8 continued on next page

Figure 8 continued

of ISRE-associated genes. FLCN^{KO} RPTEC cells show both upregulation of E-box and ISRE-associated genes. Expression levels were determined by qPCR and are representative of two independent experiments. To determine quantitative gene expression data, levels were normalized to the geometric mean of two housekeeping genes. See ***Figure 8—source data 1*** for raw qRT-PCR values and fold change calculations. (**B**) Western blots of subcellular fractions show enhanced binding of TFE3 to DNA in FLCN^{NEG} RPTEC and SFPQ-TFE3 RPTEC. STAT2 DNA-binding was enhanced upon FLCN loss but reduced by SFPQ-TFE3 over-expression in RPTEC. STAT2 was blotted on separate blots of the same lysates. Histone H3 levels were used as loading control and as marker for chromatin fraction. Western blot was performed two times, using independent fractionations. (**C**) Colony formation assays show that loss of FLCN in wild-type or SFPQ-TFE3 RPTEC reduces colony outgrowth. SFPQ-TFE3 RPTEC show more colonies than wild type RPTEC after 10 days. Insets show bright field images (×20 magnification). Cells were seeded in three technical replicates and experiment was performed twice. (**D**) Loss of FLCN in RPTEC results in slower growth, which is reverted when FLCN expression is restored by over-expression. Cell lines were seeded in equal densities and total cell numbers were counted three times within 11 days. Results shown are representative for two independent experiments. (**E**) Treatment with IFNγ (100IU/ml) or combining FLCN^{KO} in SFPQ-TFE3 RPTEC results in growth inhibition. Cell lines were seeded in equal densities and total cell number was counted twice within 7 days. Results shown are representative for two independent experiments. The growth curve of FLCN^{KO} RPTEC (**D**) is added for comparison.

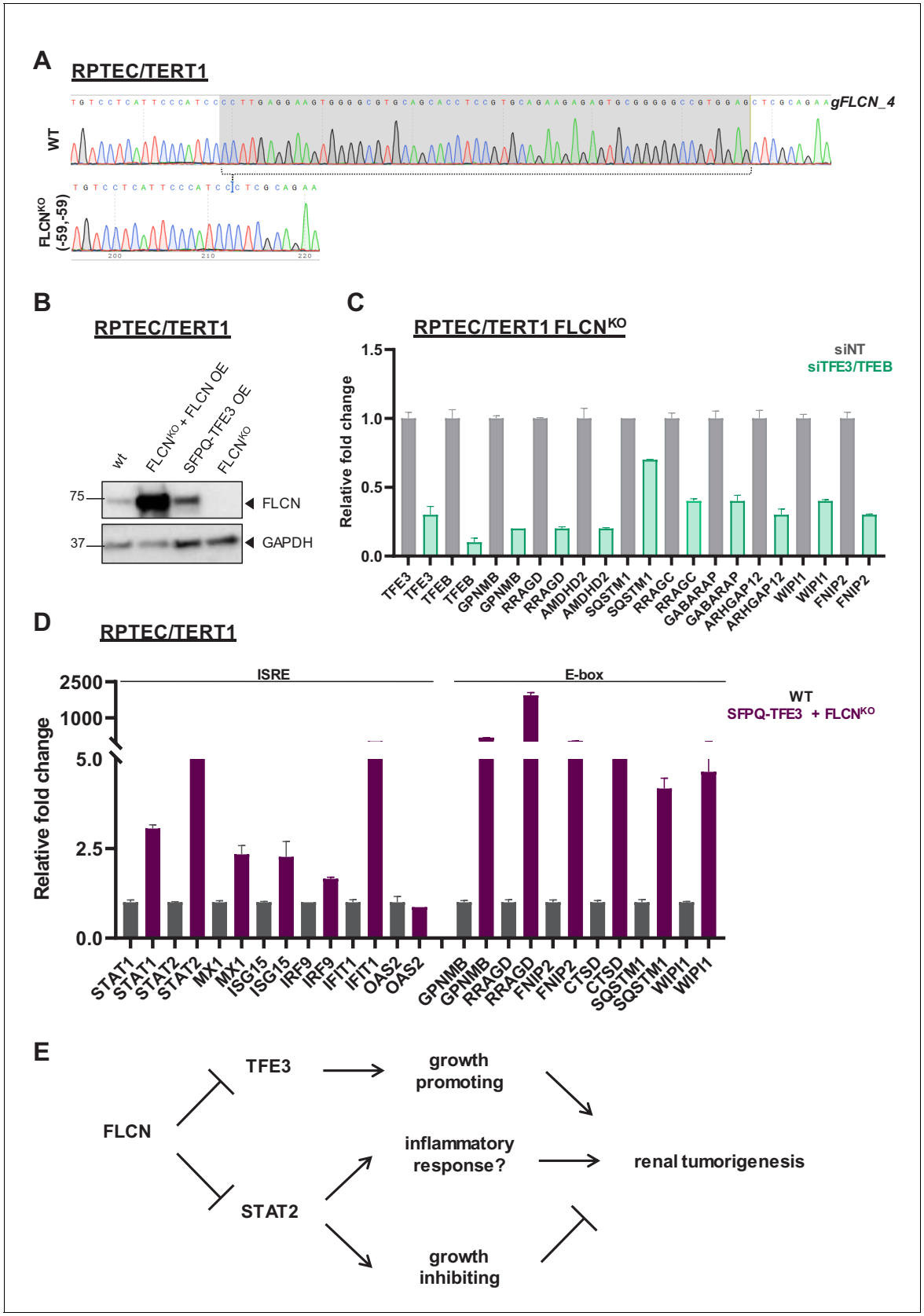

Figure 8—figure supplement 1. Creation and validation of FLCN^{NEG} and SFPQ-TFE3 RPTECs. (**A**) Validation of FLCN knock out in RPTEC by sequencing. Alignment of Sanger sequence chromatograms of FLCN^{WT} and FLCN^{KO} RPTEC cell line reveals homozygous deletion of 59 nucleotides in

Figure 8—figure supplement 1 continued on next page

Figure 8—figure supplement 1 continued

the diploid FLCN^{KO} clone. (**B**) Western blot of FLCN expression levels in wild-type, FLCN re-expression (OE), SFPQ-TFE3, and FLCN^{KO} RPTEC/TERT1 cell lines. GAPDH was used as loading control. (**C**) Knock down of TFE3/TFEB (siRNA, 10 nM, 72 hr) dampens the TFE expression gene signature induced in RPTEC FLCN^{KO} cells. Expression levels were determined by qRT-PCR and are normalized to siNT and representative of three independent experiments. To determine quantitative gene expression levels the data were normalized to the geometric mean of two housekeeping genes. See ***Figure 8—source data 1*** for raw qRT-PCR values and fold change calculations. (**D**) Combining SFPQ-TFE3 with FLCN^{KO} in RPTEC results in upregulation of ISRE-associated genes as well as high expression of E-box target genes. Expression levels were determined by qPCR and are representative of two independent experiments. See ***Figure 8—source data 1*** for raw qRT-PCR values and fold change calculations. (**E**) Diagram depicting our hypothesis that FLCN loss may induces a STAT2-mediated IFN signature which results in growth inhibition, counteracting the growth promoting function of constitutive activation of TFE3 in renal cells. Alternatively, a constitutively upregulated IFN signature may ultimately contribute to an inflammatory response that promotes tumorigenesis.

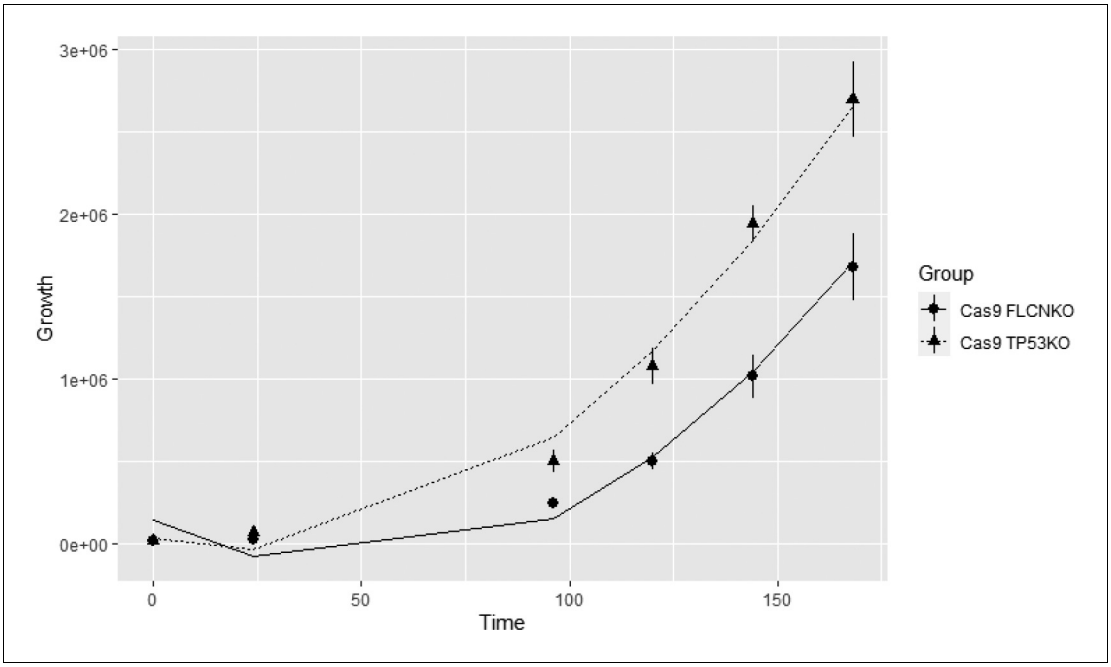

Scheme 1. Growth curves of FLCNKO and TP53KO with the fitted curves.